

Second-order sensitivity of parallel shear flows and optimal spanwise-periodic flow modifications

E. Boujo, A. Fani and F. Gallaire

LFMI, École Polytechnique Fédérale de Lausanne, CH-1015 Lausanne, Switzerland

(Received ?; revised ?; accepted ?. - To be entered by editorial office)

We perform a second-order sensitivity analysis of the linear temporal stability of a parallel mixing layer $U_0(y)$ subject to small spanwise-periodic modification $\epsilon U_1(y) \cos(\beta z)$. It is known that spanwise-periodic flow modifications have a quadratic effect on the stability properties of parallel flows (i.e. the first-order eigenvalue variation is zero), hence the need for a second-order analysis. From a simple one-dimensional (1D) calculation we compute the second-order sensitivity operator, which allows us to predict the effect on stability of any $U_1(y)$ without computing the eigenmode correction. Comparisons with two-dimensional (2D) stability calculations of modified flows show excellent agreement.

From the second-order sensitivity operator we optimise the growth rate variation and compute the most stabilising and most destabilising U_1 , together with lower and upper bounds for the growth rate variation induced by any spanwise-periodic modification of given amplitude ϵ . These bounds show a local maximum for a spanwise wavenumber of order unity $\beta \simeq 1$, while they diverge like β^{-2} as β goes to zero (long-wavelength limit). The most stabilising (destabilising) U_1 determined for the most unstable streamwise wavenumber α_{max} is efficient in stabilising (destabilising) the flow for other values of α too. We also find that optimal 2D spanwise-periodic flow modifications are more efficient in stabilising (destabilising) than the optimal 1D spanwise-invariant modification provided the amplitude ϵ and wavelength $2\pi/\beta$ are large enough.

Key words: hydrodynamic instability, shear layers, flow control

1. Introduction

It is well known that the addition of three-dimensional (3D) spanwise-periodic perturbations to a two-dimensional (2D) cylinder wake can greatly alter the flow and can in particular stabilise vortex shedding (Zdravkovich 1981; Kim & Choi 2005; Choi *et al.* 2008). Recently, Hwang *et al.* (2013) proposed an explanation of this effect based on the linear stability of the spanwise modulated parallel wake flow. They demonstrated a substantial attenuation of the absolute instability growth rate in a range of wavelengths corresponding to results from experiments and direct numerical simulation.

In a recent paper, Del Guercio *et al.* (2014) showed that suitable spanwise-periodic perturbations added to nominally parallel wakes significantly reduce the temporal stability growth rate of the inflectional instability and completely quench the absolute instability as well. Perturbations to the nominally parallel base flow were chosen as the non-linear streaks resulting from the optimal lift-up mechanism, i.e. the transient growth of optimal streamwise-uniform spanwise-periodic vortices. The absolute and maximum

temporal growth rates were found to depend quadratically on the streak amplitudes, as suggested by Hwang *et al.* (2013) who demonstrated that the first-order linear sensitivity was zero for spanwise-periodic disturbances of the base flow.

Cossu (2014) outlined a rigorous mathematical procedure to compute beforehand the quadratic (second-order) sensitivity of an eigenmode when its linear (first-order) sensitivity vanishes. He used this method to explain the stabilisation of global modes of the one-dimensional (1D) Ginzburg-Landau equation, serving as a model equation for spatially developing shear flows submitted to spanwise-periodic modulations. Tammisola *et al.* (2014) applied a similar technique to investigate the stabilisation of the 2D wake behind a flat plate using spanwise-periodic wall actuation. In these two studies, *particular* base flow modifications were prescribed and the resulting first-order eigenmode variations had to be computed explicitly to obtain the eigenvalue variations.

In this paper, we address the question of *optimal* spanwise-periodic flow modification. In addition to using an asymptotic expansion to express the second-order eigenvalue variation, we determine a second-order sensitivity operator which allows us to predict the eigenvalue variation resulting from *any* base flow modification without ever computing the first-order eigenmode correction. Further, we optimise the eigenvalue variation and obtain *optimal* flow modifications, i.e. the most stabilising and most destabilising spanwise-periodic base flow modulations.

We focus on the classical hydrodynamic stability of nominally parallel shear flows, governed by the linearised Navier-Stokes (NS) equations at finite Reynolds number Re (the so-called Orr-Sommerfeld equations). A normal mode expansion yields a set of eigenvalues and eigenmodes for any given streamwise wavenumber α . In the prototypical hyperbolic-tangent shear layer flow, there exists a finite band of wavenumbers where one (and only one) mode is unstable when Re is beyond an $\mathcal{O}(10)$ critical value. We consider base flow modifications that are unidirectional and parallel to the base flow direction, and spanwise-periodic of wavenumber β . Using the closed-form expression of the second-order sensitivity, we optimise the eigenvalue variation for any wavenumber pair (α, β) , thus obtaining optimal base flow modifications together with bounds for the largest possible growth rate decrease and increase.

2. Problem formulation

2.1. Second-order eigenvalue variation

Consider a generic 1D parallel flow $U_0(y)\mathbf{e}_x$ perturbed with a 2D spanwise-periodic modification of small amplitude ϵ :

$$\mathbf{U}(y, z) = (U_0(y) + \epsilon U_1(y) \cos(\beta z)) \mathbf{e}_x. \quad (2.1)$$

Assuming a normal mode expansion $\hat{\mathbf{q}}(x, y, z, t) = \mathbf{q}(y, z) \exp(i\alpha x + \lambda t)$ in spanwise coordinate x and time t for small-amplitude perturbations $\hat{\mathbf{q}} = (\hat{\mathbf{u}}, \hat{p})^T = (\hat{u}, \hat{v}, \hat{w}, \hat{p})^T$ and linearising the NS equations results in the eigenvalue problem

$$\lambda \mathbf{u} + \mathbf{U} \cdot \nabla \mathbf{u} + \mathbf{u} \cdot \nabla \mathbf{U} + \nabla p - Re^{-1} \nabla^2 \mathbf{u} = \mathbf{0}, \quad \nabla \cdot \mathbf{u} = 0 \quad (2.2)$$

for the eigenvalue $\lambda = \lambda_r + i\lambda_i$. The set of growth rates λ_r and frequencies λ_i determine the linear temporal stability properties of the flow.

While it is common at this stage, for spanwise-invariant parallel base flows, to transform the primitive variables $\mathbf{q} = (\mathbf{u}, p)^T$ into the Orr-Sommerfeld variables (cross-stream velocity and vorticity), we keep here the primitive variables and write (2.2) formally as $\lambda \mathbf{E} \mathbf{q} + \mathbf{A} \mathbf{q} = \mathbf{0}$. Since the linearised NS operator \mathbf{A} is linear in the base flow \mathbf{U} , it can be

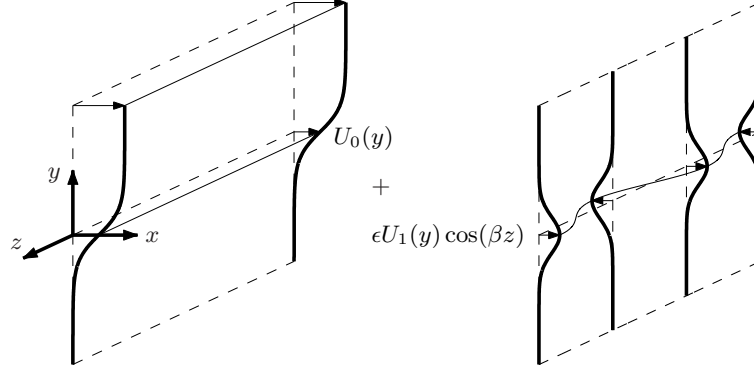


FIGURE 1. Sketch of the base flow configuration: a 1D parallel flow $U_0(y)$ is modified with a small amplitude 2D spanwise-periodic flow $\epsilon U_1(y) \cos(\beta z)$.

expanded exactly to arbitrary order (here to second order) as $\mathbf{A} = \mathbf{A}_0 + \epsilon \mathbf{A}_1$. The singular matrix \mathbf{E} need not be expanded since it does not depend on the base flow. Detailed expressions of all operators are given in Appendix A. Note in particular that \mathbf{A}_0 depends on the unperturbed base flow U_0 , and \mathbf{A}_1 depends on the base flow modification U_1 .

We look for perturbed eigenvalues and eigenmodes using the following expansion in the amplitude ϵ of the base flow modification:

$$\lambda = \lambda_0 + \epsilon \lambda_1 + \epsilon^2 \lambda_2 + \dots, \quad \mathbf{q} = \mathbf{q}_0 + \epsilon \mathbf{q}_1 + \epsilon^2 \mathbf{q}_2 + \dots \quad (2.3)$$

Substituting (2.3) into (2.2), we recover at leading order (ϵ^0) the linearised NS equations

$$\lambda_0 \mathbf{u}_0 + \mathbf{U}_0 \cdot \nabla \mathbf{u}_0 + \mathbf{u}_0 \cdot \nabla \mathbf{U}_0 + \nabla p_0 - Re^{-1} \nabla^2 \mathbf{u}_0 = \mathbf{0}, \quad \nabla \cdot \mathbf{u}_0 = 0, \quad (2.4)$$

which we write as an eigenvalue problem for the eigenvalue λ_0 and eigenmode \mathbf{q}_0 :

$$(\lambda_0 \mathbf{E} + \mathbf{A}_0) \mathbf{q}_0 = \mathbf{0}. \quad (2.5)$$

In the following we focus on the leading (most unstable) eigenvalue and its associated eigenmode, which is 2D for inflectional velocity profiles: $\partial_z \mathbf{q}_0 = \mathbf{0}$, $w_0 = 0$.

At first order (ϵ^1) we obtain

$$(\lambda_0 \mathbf{E} + \mathbf{A}_0) \mathbf{q}_1 + (\lambda_1 \mathbf{E} + \mathbf{A}_1) \mathbf{q}_0 = \mathbf{0}. \quad (2.6)$$

We introduce the following 1D and 2D Hermitian inner products

$$(\mathbf{a} | \mathbf{b}) = \lim_{L_y \rightarrow \infty} \int_{-L_y/2}^{L_y/2} \bar{\mathbf{a}} \cdot \mathbf{b} dy, \quad ((\mathbf{a} | \mathbf{b})) = \lim_{L_z \rightarrow \infty} \frac{1}{L_z} \int_{-L_z/2}^{L_z/2} (\mathbf{a} | \mathbf{b}) dz. \quad (2.7)$$

For any operator \mathbf{N} we note \mathbf{N}^\dagger the adjoint operator such that $((\mathbf{a} | \mathbf{N} \mathbf{b})) = ((\mathbf{N}^\dagger \mathbf{a} | \mathbf{b})) \forall \mathbf{a}, \mathbf{b}$. We obtain the first-order eigenvalue variation λ_1 by projecting (2.6) on the leading adjoint eigenmode \mathbf{q}_0^\dagger defined by $(\bar{\lambda}_0 \mathbf{E} + \mathbf{A}_0^\dagger) \mathbf{q}_0^\dagger = \mathbf{0}$ and normalised with $(\mathbf{q}_0^\dagger | \mathbf{E} \mathbf{q}_0) = 1$ (Hinch 1991; Trefethen *et al.* 1993; Chomaz 2005; Giannetti & Luchini 2007):

$$\lambda_1 = - \left((\mathbf{q}_0^\dagger | \mathbf{A}_1 \mathbf{q}_0) \right). \quad (2.8)$$

Since \mathbf{A}_1 is periodic in z , the inner product in (2.8) vanishes and the first-order eigenvalue variation is zero: $\lambda_1 = 0$. In other words, spanwise-periodic flow modifications have no first-order effect on stability properties (Hwang *et al.* 2013; Del Guercio *et al.* 2014; Cossu 2014). From (2.6), the leading eigenmode variation is $\mathbf{q}_1 = -(\lambda_0 \mathbf{E} + \mathbf{A}_0)^{-1} \mathbf{A}_1 \mathbf{q}_0$.

In this expression the operator $(\lambda_0 \mathbf{E} + \mathbf{A}_0)$ is not invertible in general since (2.5) has a non-trivial solution, but the inverse is taken in the subspace orthogonal to \mathbf{q}_0 , and \mathbf{q}_1 is defined up to any constant component in the direction of \mathbf{q}_0 (Hinch 1991). This is made possible by the solvability condition (Fredholm theorem) for (2.6) being satisfied: the forcing term $(\lambda_0 \mathbf{E} + \mathbf{A}_1)\mathbf{q}_0 = \mathbf{A}_1\mathbf{q}_0$ is orthogonal to the solution \mathbf{q}_0^\dagger of the adjoint equation associated with (2.5), as expressed precisely by (2.8).

At second order (ϵ^2) we obtain $(\lambda_0 \mathbf{E} + \mathbf{A}_0)\mathbf{q}_2 + \mathbf{A}_1\mathbf{q}_1 + \lambda_2 \mathbf{E}\mathbf{q}_0 = \mathbf{0}$, which yields after projection on the leading adjoint eigenmode:

$$\lambda_2 = - \left(\left(\mathbf{q}_0^\dagger \mid \mathbf{A}_1 \mathbf{q}_1 \right) \right) = \left(\left(\mathbf{q}_0^\dagger \mid \mathbf{A}_1 (\lambda_0 \mathbf{E} + \mathbf{A}_0)^{-1} \mathbf{A}_1 \mathbf{q}_0 \right) \right). \quad (2.9)$$

For a *given* flow modification U_1 , one can explicitly compute the modification \mathbf{A}_1 of the linearised NS operator and use (2.9) to obtain the second-order eigenvalue variation. However, in order to investigate the effect of *any* flow modification, it is desirable to manipulate this expression to isolate a sensitivity operator independent of U_1 , similar to classical first-order sensitivity analyses (Hill 1992; Marquet *et al.* 2008; Meliga *et al.* 2010). We use adjoint operators to perform this manipulation in section 2.2.

2.2. Second-order sensitivity

We look for a sensitivity operator \mathbf{S}_2 such that the second-order eigenvalue variation induced by any small spanwise-periodic flow modification $\mathbf{U}_1 = U_1(y) \cos(\beta z) \mathbf{e}_x$ as given in (2.1) is easily predicted by the inner product

$$\lambda_2 = ((U_1 \mid \mathbf{S}_2 U_1)). \quad (2.10)$$

We rewrite (2.9) as $\lambda_2 = \left(\left(\mathbf{A}_1^\dagger \mathbf{q}_0^\dagger \mid (\lambda_0 \mathbf{E} + \mathbf{A}_0)^{-1} \mathbf{A}_1 \mathbf{q}_0 \right) \right)$ and, given that \mathbf{A}_1 is linear in U_1 , we introduce operators \mathbf{M} and \mathbf{L} such that $\mathbf{A}_1^\dagger \mathbf{q}_0^\dagger = \mathbf{M} U_1$ and $\mathbf{A}_1 \mathbf{q}_0 = \mathbf{L} U_1$ (detailed expressions in Appendix B). We finally obtain:

$$\lambda_2 = ((U_1 \mid \mathbf{M}^\dagger (\lambda_0 \mathbf{E} + \mathbf{A}_0)^{-1} \mathbf{L} U_1)) \quad (2.11)$$

At this point $\mathbf{S}_2 = \mathbf{M}^\dagger (\lambda_0 \mathbf{E} + \mathbf{A}_0)^{-1} \mathbf{L}$ depends on z , but (2.11) only contains terms proportional to $\cos^2(\beta z)$ and $\sin^2(\beta z)$ and can therefore be replaced with

$$\lambda_2 = (U_1 \mid \tilde{\mathbf{S}}_2 U_1) = \left(U_1 \mid \frac{1}{2} \tilde{\mathbf{M}}^\dagger (\lambda_0 \mathbf{E} + \tilde{\mathbf{A}}_0)^{-1} \tilde{\mathbf{L}} U_1 \right) \quad (2.12)$$

where $\tilde{\mathbf{M}}^\dagger$ and $\tilde{\mathbf{L}}$ are z -independent versions of \mathbf{M}^\dagger and \mathbf{L} , and z -derivatives in \mathbf{A}_0 are appropriately replaced with β terms in $\tilde{\mathbf{A}}_0$ (see also Appendix C):

$$\tilde{\mathbf{M}}^\dagger = \left[i\alpha \bar{u}_0^\dagger, i\alpha \bar{v}_0^\dagger - \partial_y \bar{u}_0^\dagger - \bar{u}_0^\dagger \partial_y, -\beta \bar{u}_0^\dagger, 0 \right], \quad \tilde{\mathbf{L}} = [i\alpha u_0 + v_0 \partial_y, i\alpha v_0, 0, 0]^T, \quad (2.13)$$

$$\tilde{\mathbf{A}}_0 = \begin{bmatrix} i\alpha U_0 - Re^{-1} \nabla_{\alpha\beta} & \partial_y U_0 & 0 & i\alpha \\ 0 & i\alpha U_0 - Re^{-1} \nabla_{\alpha\beta} & 0 & \partial_y \\ 0 & 0 & i\alpha U_0 - Re^{-1} \nabla_{\alpha\beta} & -\beta \\ i\alpha & \partial_y & \beta & 0 \end{bmatrix}, \quad (2.14)$$

$\nabla_{\alpha\beta} = -\alpha^2 + \partial_{yy} - \beta^2$, yielding the z -independent sensitivity $\tilde{\mathbf{S}}_2 = \frac{1}{2} \tilde{\mathbf{M}}^\dagger (\lambda_0 \mathbf{E} + \tilde{\mathbf{A}}_0)^{-1} \tilde{\mathbf{L}}$.

An important difference with first-order sensitivity analysis is that λ_1 ($\neq 0$ in general) depends linearly on U_1 , while here λ_2 depends quadratically on U_1 . As a consequence, in the case of first-order sensitivity, one can investigate the effect of any base flow modification in a very convenient way: since $\lambda_1 = (\mathbf{S}_1 \mid \mathbf{U}_1)$ is linear in \mathbf{U}_1 , a linear combination of flow modifications results in the same linear combination of eigenvalue variations. In

particular, any \mathbf{U}_1 can be decomposed into a combination of flow modifications localised in \mathbf{x}_c (e.g. Gaussian functions approximating pointwise Dirac delta functions), each of them resulting into an individual eigenvalue variation obtained from the sensitivity at \mathbf{x}_c only; since \mathbf{S}_1 is a vector field, it is easily visualised with a map, and one can identify most sensitive regions at a glance (Marquet *et al.* 2008; Meliga *et al.* 2010).

In contrast, in the case of second-order sensitivity, $\lambda_2 = (\mathbf{U}_1 | \mathbf{S}_2 \mathbf{U}_1)$ depends quadratically on \mathbf{U}_1 , and a linear combination of base flow modifications does *not* result in the same combination of eigenvalue variations, not to mention quadratic coupling effects between different components U_1, V_1, W_1 (as appears clearly in the alternative expression $\lambda_2 = (\mathbf{U}_1 \mathbf{U}_1^T) : \mathbf{S}_2$ denoting the inner product of \mathbf{S}_2 with the tensor $\mathbf{U}_1 \mathbf{U}_1^T$). Furthermore, the sensitivity operator \mathbf{S}_2 is a tensor field, whose visualisation would require an impractically large number of maps. Tammisola *et al.* (2014) proposed to identify sensitive regions with maps showing the effect of a specific base flow modification (localised Gaussian U_1 , and $V_1 = W_1 = 0$) applied successively in all locations of the domain, essentially reproducing systematic traversing experimental measurements. We prefer taking advantage of knowing the sensitivity operator \mathbf{S}_2 , and we show in section 2.3 how to extract *optimal* flow modifications resulting in maximal eigenvalue variation.

2.3. Optimal flow modification

The second-order sensitivity operator is useful in that it predicts the leading eigenvalue variation resulting from any U_1 without the need to solve the eigenvalue problem for the modified flow. In addition, it allows one to determine the largest possible eigenvalue variation for all modifications of given amplitude. Specifically, the largest increase (decrease) in growth rate to be expected for a modification of unit norm $\|U_1\| = (U_1 | U_1)^{1/2} = 1$ is the largest positive (largest negative) eigenvalue of the symmetric real part of $\tilde{\mathbf{S}}_2$:

$$\max_{\|U_1\|=1} \lambda_{2r} = \max_{\|U_1\|=1} \left(U_1 | \frac{1}{2} (\tilde{\mathbf{S}}_{2r} + \tilde{\mathbf{S}}_{2r}^T) U_1 \right) = \lambda_{max} \left\{ \frac{1}{2} (\tilde{\mathbf{S}}_{2r} + \tilde{\mathbf{S}}_{2r}^T) \right\}, \quad (2.15a)$$

$$\min_{\|U_1\|=1} \lambda_{2r} = \min_{\|U_1\|=1} \left(U_1 | \frac{1}{2} (\tilde{\mathbf{S}}_{2r} + \tilde{\mathbf{S}}_{2r}^T) U_1 \right) = \lambda_{min} \left\{ \frac{1}{2} (\tilde{\mathbf{S}}_{2r} + \tilde{\mathbf{S}}_{2r}^T) \right\}, \quad (2.15b)$$

where $\tilde{\mathbf{S}}_2 = \tilde{\mathbf{S}}_{2r} + i\tilde{\mathbf{S}}_{2i}$, and right-hand sides come from $\tilde{\mathbf{S}}_{2r} + \tilde{\mathbf{S}}_{2r}^T$ being real symmetric, so that the Rayleigh quotient is maximal (minimal) for the largest positive (largest negative) eigenvalue. The optimal flow modification, i.e. the most stabilising (destabilising) U_1 is the eigenmode of unit norm associated with λ_{max} (λ_{min}). Similar relations hold for the maximal shift in frequency, real parts being replaced with imaginary parts.

3. Results: the parallel mixing layer

We focus on a classical parallel flow: the hyperbolic-tangent mixing layer $U_0(y) = 1 + R \tanh(y)$ (Michalke 1964) with $R = 1$, at $Re = 100$. We solve the eigenvalue problem (2.2) in primitive variables (\mathbf{u}, p) with a 1D spectral method using Chebyshev polynomials (Trefethen 2000) on $y \in [-5; 5]$ and homogeneous Dirichlet boundary conditions on velocity components. The largest growth rate is obtained for the streamwise wavenumber $\alpha = \alpha_{max} = 0.45$, where the leading eigenvalue is $\lambda_0 = 0.1676 - 0.4500i$, in agreement with existing results (Betchov & Szewczyk 1963; Michalke 1964; Villermaux 1998).

3.1. Particular flow modifications

Figure 2 shows three profiles of flow modification $U_1(y)$ and the corresponding total flow profiles $U_0(y) + \epsilon U_1(y) \cos(\beta z)$ at spanwise stations $z = 0$ and $z = \pi/\beta$. Taking for

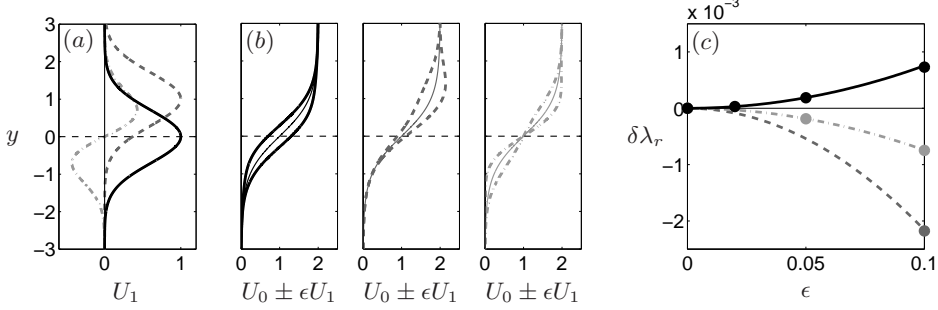


FIGURE 2. Effect of a spanwise-periodic flow modification $\epsilon U_1(y) \cos(\beta z)$ of wavenumber $\beta = 1$ on the leading eigenmode's growth rate at streamwise wavenumber $\alpha = 0.5$ for the hyperbolic-tangent parallel flow $U_0(y) = 1 + \tanh(y)$. (a) Flow modification profiles: symmetric Gaussian centred in $y = 0$ (black solid) or in $y = 1$ (dark grey dashed), antisymmetric Gaussian centred in $y = 0$ (light grey dash-dotted). (b) Total flow at $z = 0$ and $z = \pi/\beta$. (c) Growth rate variation predicted by sensitivity analysis (lines) and calculated from the full stability problem (symbols).

instance $\beta = 1$, the effect on the leading growth rate at $\alpha = 0.5$ predicted from sensitivity analysis according to (2.12) is in very good agreement with full 2D calculations conducted on modified base flows with the following method: equations (2.2) are discretised on the computational domain $y \in [-5; 5]$, $z \in [0; 2 \cdot 2\pi/\beta]$ with the finite element solver FreeFem++ (Hecht 2012) using P2 elements for velocity components and P1 elements for pressure; homogeneous Dirichlet boundary conditions $\mathbf{u} = \mathbf{0}$ are imposed on $y = \pm 5$, while periodic boundary conditions are imposed on lateral boundaries ($z = 0$, $z = 2 \cdot 2\pi/\beta$); finally the library SLEPc is used to compute generalised eigenpairs of the eigenvalue problem.

3.2. Optimal flow modifications

We compute the most destabilising and most stabilising spanwise-periodic flow modifications according to (2.15). Figure 3(a) shows the largest positive and negative second-order eigenvalue variations at $\alpha = 0.5$ as function of the spanwise wavenumber. These curves provide bounds for the largest possible destabilisation and stabilisation. Each of these two curves has a local optimum, λ_{2r}^d and λ_{2r}^s respectively, close to $\beta^d = \beta^s = 0.8$. As shown in figure 3(b), for a fixed choice of β the upper and lower bounds strongly increase with α in the unstable domain $\alpha \in [0; 1]$, indicating that the optimal flow modifications have a stronger effect on the leading eigenmode at smaller streamwise wavelengths. Figure 3(c) shows that the local optima λ_{2r}^d and λ_{2r}^s increase exponentially, while the corresponding optimal value of β becomes slightly larger but remains of order ~ 1 . For smaller values of β , the upper and lower bounds diverge like β^{-2} , pointing to a strong authority of the flow modification as its spanwise wavelength tends to infinity. This diverging effect at small β was also observed by Del Guercio *et al.* (2014) and Cossu (2014) for a specific choice of base flow modification (streaks created by optimal streamwise vortices in a 2D wake, and uniform modification in a 1D Ginzburg-Landau equation, respectively). Based on an expansion on the eigenmodes of the unperturbed problem (Hinch 1991), this phenomenon was explained by Tammisola *et al.* (2014) as a modal resonance between unperturbed eigenmodes having close eigenvalues, namely the eigenmode of interest (2D in our case) and eigenmodes whose spanwise wavenumber differ by $\pm\beta$ from that of the eigenmode of interest. If β is so small that the eigenvalue difference $\Delta\lambda$ between these modes is of order ϵ , the modal resonance results in a non-small second-order eigenvalue variation $\lambda_2 = \mathcal{O}(\epsilon/\Delta\lambda) = \mathcal{O}(1)$ and the asymptotic expansion (2.3) is not valid any longer. We show in Appendix D that the eigenvalue difference between the 2D eigenmode of interest

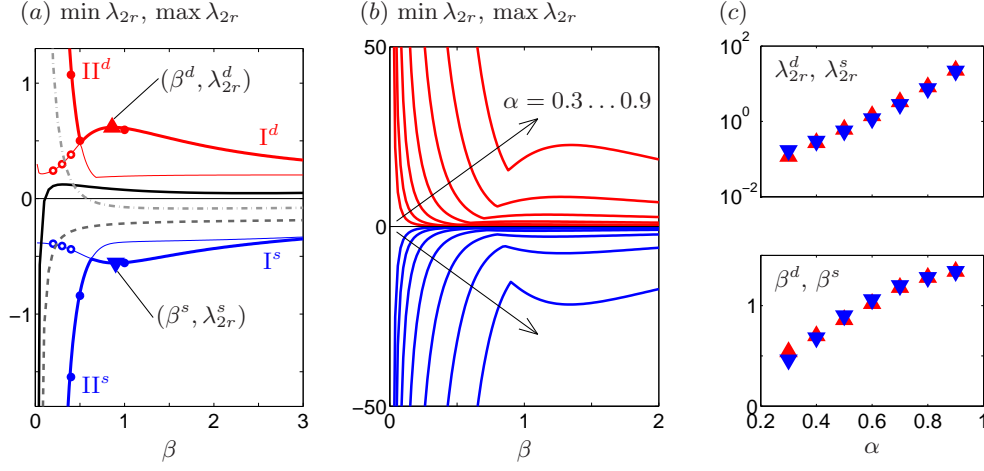


FIGURE 3. Upper and lower bounds on λ_2 , i.e. maximal stabilising (blue) and destabilising (red) effect on the leading growth rate, as predicted by sensitivity analysis. (a) $\alpha = 0.5$. Crossing of branches I and II, optimal at large and small β respectively. Circles are calculations for the full stability problem. Grey lines show sub-optimal results for the three particular profiles of figure 2. (b) Upper and lower bounds for $\alpha = 0.3 \dots 0.9$. (c) Variation with α of the local maxima and minima of shown as triangles in (a), and corresponding spanwise wavenumbers.

and eigenmodes of small spanwise wavenumber $\pm\beta$ scales precisely like β^2 , consistent with the divergence behaviour $\lambda_2 \sim \beta^{-2}$ we observed.

The upper and lower bounds in figure 3(a) are actually made of two branches which intersect and correspond to different families of flow modifications U_1 . We call branch I the optimal family at large β (corresponding to the local optima at β^d, β^s), and branch II the optimal family at small β (diverging as $\beta \rightarrow 0$). Optimal modifications are shown in figure 4 for $\alpha = \alpha_{max} = 0.45$. At smaller spanwise wavelength $\beta < 0.5$, the most destabilising U_1 is antisymmetric and the most stabilising U_1 symmetric; at larger spanwise wavelength $\beta > 0.5$, symmetry properties are exchanged as branches I and II cross.

A question of interest is whether the most stabilising flow modification obtained for $\alpha = \alpha_{max}$ is stabilising at other values of α too. In other words, is the optimisation robust? We investigate this point by computing the variation in leading growth rate predicted by (2.12) when the flow is modified with $\epsilon U_1(y) \cos(\beta z)$, where $\epsilon = 0.1$ and U_1 is chosen in branch I for $\alpha = \alpha_{max} = 0.45$. Figure 5 shows that whatever the choice of spanwise wavenumber β , flow modifications optimised to stabilise (destabilise) the leading mode at α_{max} have a stabilising (destabilising) effect at almost all other values of α too. This effect is negligible at small α , and larger at larger α . This is due to the dispersion relation at small α being independent of the details of the velocity profile: in particular, according to the Kelvin-Helmholtz dispersion relation $\lambda_r = \alpha \Delta U / 2$ pertaining to the vorticity sheet model, the growth rate is only determined by the velocity difference ΔU between the two streams. In contrast, the maximal growth rate and the cut-off wavenumber are influenced by other characteristics of the velocity profile (e.g. thickness and shear). Here, since $U_1(y)$ vanishes far from $y = 0$, it modifies neither the velocity difference $\Delta U = 2R$ nor the growth rate at small α .

3.3. Comparison with optimal 1D flow modification

Since the effect of 2D spanwise-periodic flow modifications $\epsilon U_1(y) \cos(\beta z)$ is quadratic, for small amplitudes ϵ one can expect this second-order effect $|\lambda - \lambda_0| \sim \epsilon^2$ to be overcome by the non-zero first-order effect $|\lambda - \lambda_0| \sim \epsilon$ of 1D spanwise-invariant flow modifications

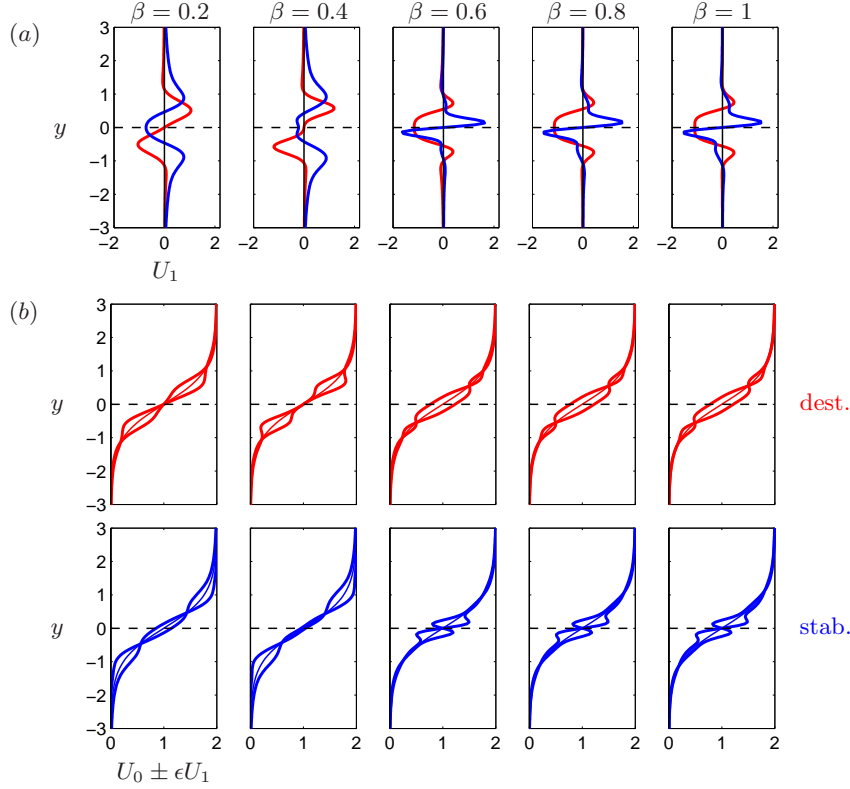


FIGURE 4. (a) Most destabilising (red) and stabilising (blue) for $\alpha = \alpha_{max} = 0.45$, $\beta = 0.2, 0.4, 0.6, 0.8, 1$. (b) Total modified flow $U_0(y) + \epsilon U_1(y) \cos(\beta z)$ at $z = 0$ and $z = \pi/\beta$ for $\epsilon = 0.2$.

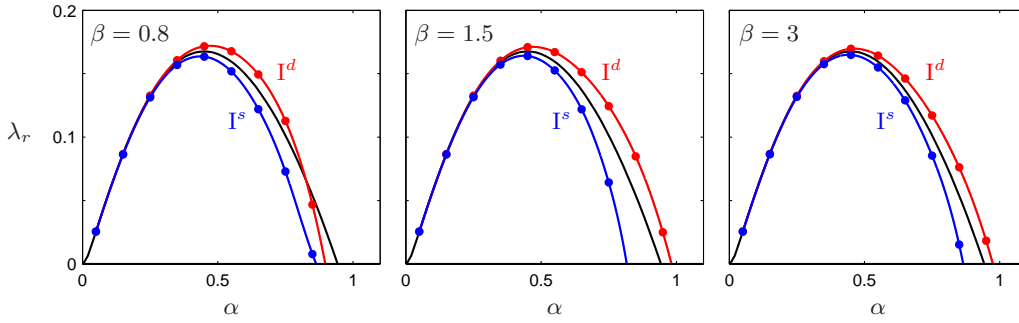


FIGURE 5. Effect of optimal spanwise-periodic flow modification $\epsilon U_1(y) \cos(\beta z)$ on the leading growth rate with U_1 optimised for $\alpha = \alpha_{max} = 0.45$ and $\beta = 0.8, 1.5, 3$. Branch I^d : most destabilising; branch I^s : most stabilising. $\epsilon = 0.1$.

$\epsilon U_1(y)$. We use first-order sensitivity (Bottaro *et al.* 2003) to compute the eigenvalue sensitivity to 1D flow modification $S_1 = \mathbf{e}_x \cdot (-\mathbf{u}_0^\dagger \cdot \nabla \mathbf{u}_0^H + \bar{\mathbf{u}}_0 \cdot \nabla \mathbf{u}_0^\dagger) = i\alpha(2\bar{u}_0 u_0^\dagger + \bar{v}_0 v_0^\dagger) + \bar{v}_0 \partial_y u_0^\dagger$, from which we deduce the optimal 1D flow modification (equal to the real part of the sensitivity itself, $U_1 = S_{1r}$) and the maximal growth rate variation, $\max \lambda_{1r} = (S_{1r} | U_1) = (S_{1r} | S_{1r})$. The optimal 1D base flow modification is depicted in figure 6(a). It is similar to the most destabilising structure at small β in figure 4(a).

We then compare the effect of optimal 1D and 2D flow modifications of unit norm *per unit spanwise length*, taking into account the actual cost of modifying the flow. For the

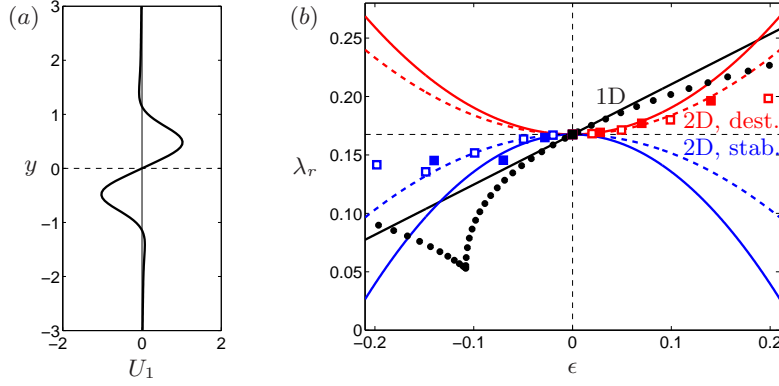


FIGURE 6. (a) Profile of the optimal 1D modification at $\alpha = \alpha_{max} = 0.45$. (b) Effect of optimal 1D (spanwise-invariant) and optimal 2D (spanwise-periodic) flow modification on the leading growth rate at $\alpha = \alpha_{max} = 0.45$. Lines: sensitivity prediction (for 2D modification, $\beta = 0.4$: solid; $\beta = 0.8$: dashed); symbols: full stability calculations.

1D base flow modification, it is enough to reverse the sign of U_1 to change a stabilising effect into a destabilising one and vice-versa, in contrast to spanwise-periodic control where stabilising and destabilising U_1 are radically different. Results at $\alpha = \alpha_{max}$ and $\beta = 0.4$ (branch II), $\beta = 0.8$ (branch I) are illustrated in figure 6(b) and show that optimal 2D spanwise-periodic flow modifications (blue and red lines) are indeed less efficient than optimal 1D modification (black line) at small amplitude, but become more efficient at larger amplitudes, for instance $|\epsilon| \geq 15 - 20\%$ when choosing $\beta = 0.4$. Exact eigenvalues computed from the full eigenvalue problem are also reported as symbols. Unlike results reported in Del Guercio *et al.* (2014), non-linear effects are significant for the optimal 1D flow modification. We observe that in the stabilising case, exact eigenvalue calculations show the existence of a mode becoming unstable under the action of base flow modification both in the 1D spanwise-uniform and 2D spanwise-periodic cases.

4. Conclusion

We have determined analytically the second-order sensitivity of the leading eigenvalue in a parallel shear flow at streamwise wavenumber α with respect to small spanwise-periodic velocity modifications of wavenumber β . The second-order sensitivity operator allowed us to obtain the eigenvalue variation induced by any such flow modification without ever calculating the first-order eigenmode correction. Predictions from sensitivity analysis have been validated against numerical calculations of the full stability problem, and a quadratic variation with the modification amplitude was recovered.

Further, for any wavenumber pair (α, β) , we have used the explicit expression of the second-order sensitivity operator to determine the most stabilising and destabilising flow modification profiles. The method readily applies to the quadratic sensitivity of the eigenmode's frequency, if one wishes for instance to detune vortex shedding frequency, and can easily be extended to other flow quantities.

We have observed that the optimally stabilising second-order sensitivity increases with α and that there exist two different branches of optimal modulations which dominate at small and large β , the former being symmetric in y and the latter antisymmetric. Optimally destabilising modulations have opposite symmetry properties.

The present analysis comes as a complement to that of Del Guercio *et al.* (2014) who

have optimised for spanwise-periodic perturbations yielding maximal transient growth, before investigating the stability of the resulting “frozen” modified flow. To be valid, such a combination of transient growth and stability analysis actually requires a separation of scales; therefore the two analyses should be combined to determine optimal forcing structures. In spatially developing flows, like cylinder wakes, a generalisation of the present approach would allow one to naturally combine in a single optimisation procedure (i) spatial transient growth in response to suitable spanwise-periodic forcing, and (ii) its effect on global stability properties. We are presently working on generalising to spatially developing flows the second-order sensitivity analysis and optimisation reported for parallel flows in this paper. In view of the quadratic dependence of the growth rate on the amplitude of the spanwise-periodic forcing in the cylinder wake (Del Guercio *et al.* 2014), this generalisation appears as a promising research direction.

Appendix A. Stability operators

We write explicitly the eigenvalue problem (2.2) for perturbations $\mathbf{q}(y, z) \exp(i\alpha x + \lambda t)$ linearised around the base flow $U(y, z)\mathbf{e}_x$:

$$\lambda u + i\alpha u U + v \partial_y U + w \partial_z U + i\alpha p - Re^{-1} \nabla_\alpha u = 0 \quad (\text{A } 1a)$$

$$\lambda v + i\alpha v U + \partial_y p - Re^{-1} \nabla_\alpha v = 0 \quad (\text{A } 1b)$$

$$\lambda w + i\alpha w U + \partial_z p - Re^{-1} \nabla_\alpha w = 0 \quad (\text{A } 1c)$$

$$i\alpha u + \partial_y v + \partial_z w = 0, \quad (\text{A } 1d)$$

where $\nabla_\alpha = -\alpha^2 + \partial_{yy} + \partial_{zz}$.

From the expansion (2.3), we find at leading order (ϵ^0) the eigenvalue problem (2.4)-(2.5) $(\lambda_0 \mathbf{E} + \mathbf{A}_0) \mathbf{q}_0 = \mathbf{0}$, where

$$\mathbf{E} = \begin{bmatrix} 1 & 0 & 0 & 0 \\ 0 & 1 & 0 & 0 \\ 0 & 0 & 1 & 0 \\ 0 & 0 & 0 & 0 \end{bmatrix}, \quad \mathbf{A}_0 = \begin{bmatrix} i\alpha U_0 - Re^{-1} \nabla_\alpha & \partial_y U_0 & 0 & i\alpha \\ 0 & i\alpha U_0 - Re^{-1} \nabla_\alpha & 0 & \partial_y \\ 0 & 0 & i\alpha U_0 - Re^{-1} \nabla_\alpha & \partial_z \\ i\alpha & \partial_y & \partial_z & 0 \end{bmatrix}. \quad (\text{A } 2)$$

At first-order (ϵ^1) we find equation (2.6) for \mathbf{q}_1 , $(\lambda_0 \mathbf{E} + \mathbf{A}_0) \mathbf{q}_1 + (\lambda_1 \mathbf{E} + \mathbf{A}_1) \mathbf{q}_0 = \mathbf{0}$, where

$$\mathbf{A}_1 = \begin{bmatrix} i\alpha U_1 \cos(\beta z) & \partial_y U_1 \cos(\beta z) & -\beta U_1 \sin(\beta z) & 0 \\ 0 & i\alpha U_1 \cos(\beta z) & 0 & 0 \\ 0 & 0 & i\alpha U_1 \cos(\beta z) & 0 \\ 0 & 0 & 0 & 0 \end{bmatrix}. \quad (\text{A } 3)$$

Appendix B. Sensitivity operators

The second-order eigenvalue variation (2.10) is manipulated in order to separate the base flow modification and the second-order sensitivity operator: $\lambda_2 = ((U_1 | \mathbf{S}_2 U_1))$. To this aim, we introduce the adjoint operator \mathbf{A}_1^\dagger such that

$$\lambda_2 = \left(\left(\mathbf{q}_0^\dagger \middle| \mathbf{A}_1 (\lambda_0 \mathbf{E} + \mathbf{A}_0)^{-1} \mathbf{A}_1 \mathbf{q}_0 \right) \right) = \left(\left(\mathbf{A}_1^\dagger \mathbf{q}_0^\dagger \middle| (\lambda_0 \mathbf{E} + \mathbf{A}_0)^{-1} \mathbf{A}_1 \mathbf{q}_0 \right) \right), \quad (\text{B } 1)$$

and we isolate the flow modification by rewriting $\mathbf{A}_1^\dagger \mathbf{q}_0^\dagger = \mathbf{M}U_1$ and $\mathbf{A}_1 \mathbf{q}_0 = \mathbf{L}U_1$, where

$$\mathbf{M} = \begin{bmatrix} -i\alpha u_0^\dagger \cos(\beta z) \\ (u_0^\dagger \partial_y - i\alpha v_0^\dagger) \cos(\beta z) \\ -\beta u_0^\dagger \sin(\beta z) \\ 0 \end{bmatrix}, \quad \mathbf{L} = \begin{bmatrix} (i\alpha u_0 + v_0 \partial_y) \cos(\beta z) \\ i\alpha v_0 \cos(\beta z) \\ 0 \\ 0 \end{bmatrix}. \quad (\text{B } 2)$$

Finally the second-order eigenvalue variation reads

$$\lambda_2 = ((\mathbf{M}U_1 | (\lambda_0 \mathbf{E} + \mathbf{A}_0)^{-1} \mathbf{L}U_1)) = ((U_1 | \mathbf{M}^\dagger (\lambda_0 \mathbf{E} + \mathbf{A}_0)^{-1} \mathbf{L}U_1)), \quad (\text{B } 3)$$

where

$$\mathbf{M}^\dagger = [i\alpha \bar{u}_0^\dagger \cos(\beta z), (i\alpha \bar{v}_0^\dagger - \partial_y \bar{u}_0^\dagger - \bar{u}_0^\dagger \partial_y) \cos(\beta z), -\beta \bar{u}_0^\dagger \sin(\beta z), 0], \quad (\text{B } 4)$$

and we identify the second-order sensitivity operator $\mathbf{S}_2 = \mathbf{M}^\dagger (\lambda_0 \mathbf{E} + \mathbf{A}_0)^{-1} \mathbf{L}$.

Appendix C. Transformation to spanwise-independent operators

We give details about the simplification of the second-order sensitivity operator, from its general expression \mathbf{S}_2 (2.12) to the z -independent form $\tilde{\mathbf{S}}_2$ (2.13), which is made possible by the explicit expressions of \mathbf{M}^\dagger and \mathbf{L} being available.

We note $\mathbf{a} = (a_u, a_v, a_w, a_p)^T$ a solution of $(\lambda_0 \mathbf{E} + \mathbf{A}_0) \mathbf{a} = \mathbf{L}U_1$:

$$(\lambda_0 + i\alpha U_0 - Re^{-1} \nabla_\alpha) a_u + \partial_y U_0 a_v + i\alpha a_p = \cos(\beta z) (i\alpha u_0 + v_0 \partial_y) U_1 \quad (\text{C } 1a)$$

$$(\lambda_0 + i\alpha U_0 - Re^{-1} \nabla_\alpha) a_v + \partial_y a_p = \cos(\beta z) i\alpha v_0 U_1 \quad (\text{C } 1b)$$

$$(\lambda_0 + i\alpha U_0 - Re^{-1} \nabla_\alpha) a_w + \partial_z a_p = 0 \quad (\text{C } 1c)$$

$$i\alpha a_u + \partial_y a_v + \partial_z a_w = 0. \quad (\text{C } 1d)$$

A close inspection reveals that this solution is necessarily of the form

$$\mathbf{a} = (\tilde{a}_u \cos(\beta z), \tilde{a}_v \cos(\beta z), \tilde{a}_w \sin(\beta z), \tilde{a}_p \cos(\beta z))^T. \quad (\text{C } 2)$$

Therefore, the second-order eigenvalue variation reads

$$\lambda_2 = ((U_1 | \mathbf{S}_2 U_1)) = ((U_1 | \mathbf{M}^\dagger (\lambda_0 \mathbf{E} + \mathbf{A}_0)^{-1} \mathbf{L}U_1)) = ((U_1 | \mathbf{M}^\dagger \mathbf{a})) \quad (\text{C } 3a)$$

$$= \left((U_1 | \left(i\alpha \bar{u}_0^\dagger \tilde{a}_u + (i\alpha \bar{v}_0^\dagger - \partial_y \bar{u}_0^\dagger - \bar{u}_0^\dagger \partial_y) \tilde{a}_v \right) \cos^2(\beta z) - \beta \bar{u}_0^\dagger \tilde{a}_w \sin^2(\beta z) \right) \right) \quad (\text{C } 3b)$$

$$= \frac{1}{2} \left(U_1 | \left(i\alpha \bar{u}_0^\dagger \tilde{a}_u + (i\alpha \bar{v}_0^\dagger - \partial_y \bar{u}_0^\dagger - \bar{u}_0^\dagger \partial_y) \tilde{a}_v \right) - \beta \bar{u}_0^\dagger \tilde{a}_w \right) \quad (\text{C } 3c)$$

where the last equality comes from the integrals of $\cos^2(\beta z)$ and $\sin^2(\beta z)$ over one spanwise wavelength being equal to π/β , yielding 1/2 when normalised by the wavelength. Finally the second-order sensitivity operator becomes independent of z :

$$\lambda_2 = \left(U_1 | \frac{1}{2} \tilde{\mathbf{M}}^\dagger (\lambda_0 \mathbf{E} + \tilde{\mathbf{A}}_0)^{-1} \tilde{\mathbf{L}} U_1 \right), \quad (\text{C } 4)$$

where

$$\tilde{\mathbf{M}}^\dagger = [i\alpha \bar{u}_0^\dagger, i\alpha \bar{v}_0^\dagger - \partial_y \bar{u}_0^\dagger - \bar{u}_0^\dagger \partial_y, -\beta \bar{u}_0^\dagger, 0], \quad \tilde{\mathbf{L}} = \begin{bmatrix} i\alpha u_0 + v_0 \partial_y \\ i\alpha v_0 \\ 0 \\ 0 \end{bmatrix}, \quad (\text{C } 5)$$

$$\tilde{\mathbf{A}}_0 = \begin{bmatrix} i\alpha U_0 - Re^{-1}\nabla_{\alpha\beta} & \partial_y U_0 & 0 & i\alpha \\ 0 & i\alpha U_0 - Re^{-1}\nabla_{\alpha\beta} & 0 & \partial_y \\ 0 & 0 & i\alpha U_0 - Re^{-1}\nabla_{\alpha\beta} & -\beta \\ i\alpha & \partial_y & \beta & 0 \end{bmatrix}, \quad (\text{C } 6)$$

and $\nabla_{\alpha\beta} = -\alpha^2 + \partial_{yy} - \beta^2$.

Appendix D. Scaling in the small- β limit

Consider the unperturbed base flow and the corresponding unstable 2D eigenmode \mathbf{q}_0 solution of the eigenvalue problem $(\lambda_0 \mathbf{E} + \mathbf{A}_0)\mathbf{q}_0 = \mathbf{0}$. There also exist 3D eigenmodes of spanwise wavenumber $\beta \neq 0$, which are all less unstable. For small values of the spanwise wavenumber $|\beta| \ll 1$, the eigenvalue varies like $\lambda(\beta) \simeq \lambda_0 - C\beta^2$, $C > 0$, as outlined in the following: we estimate the eigenvalue variation for a small change of spanwise wavenumber from $\beta = 0$ to $\beta \ll 1$ by using the classical expression of first-order eigenvalue variation $\delta\lambda = -\left(\mathbf{q}_0^\dagger \middle| \delta\mathbf{A}_0 \mathbf{q}_0\right) / \left(\mathbf{q}_0^\dagger \middle| \mathbf{E} \mathbf{q}_0\right)$ where the variation of the linearised Navier-Stokes operator in this case is given by

$$\delta\mathbf{A}_0 = \begin{bmatrix} Re^{-1}\beta^2 & 0 & 0 & 0 \\ 0 & Re^{-1}\beta^2 & 0 & 0 \\ 0 & 0 & Re^{-1}\beta^2 & i\beta \\ 0 & 0 & i\beta & 0 \end{bmatrix}, \quad (\text{D } 1)$$

and therefore $\delta\lambda = Re^{-1}\beta^2$.

When the base flow is perturbed with a spanwise-periodic modification of long wavelength (small β), there is interaction between the unperturbed 2D eigenmode of interest and the unperturbed 3D eigenmodes of spanwise wavenumber $\pm\beta$, as described by Tammisola *et al.* (2014); the resonance effect these authors proposed to explain large second-order sensitivity at small β therefore leads in the present case to the second-order eigenvalue variation $|\lambda_2| \sim |\delta\lambda|^{-1} \sim \beta^{-2}$, as observed in section 3.2.

REFERENCES

- BETCHOV, R. & SZEWCZYK, A. 1963 Stability of a shear layer between parallel streams. *Physics of Fluids (1958-1988)* **6** (10), 1391–1396.
- BOTTARO, A., CORBETT, P. & LUCHINI, P. 2003 The effect of base flow variation on flow stability. *Journal of Fluid Mechanics* **476**, 293–302.
- CHOI, H., JEON, W.-P. & KIM, J. 2008 Control of flow over a bluff body. *Annual Review of Fluid Mechanics* **40**, 113–139.
- CHOMAZ, J.M. 2005 Global instabilities in spatially developing flows: Non-normality and non-linearity. *Annual Review of Fluid Mechanics* **37**, 357–392.
- COSSU, C. 2014 On the stabilizing mechanism of 2D absolute and global instabilities by 3D streaks. *ArXiv e-prints*.
- DEL GUERCIO, G., COSSU, C. & PUJALS, G. 2014 Stabilizing effect of optimally amplified streaks in parallel wakes. *Journal of Fluid Mechanics* **739**, 37–56.
- GIANNETTI, F. & LUCHINI, P. 2007 Structural sensitivity of the first instability of the cylinder wake. *Journal of Fluid Mechanics* **581**, 167–197.
- HECHT, F. 2012 New development in FreeFem++. *Journal of Numerical Mathematics* **20** (3-4), 251–265.
- HILL, D. C. 1992 A theoretical approach for analyzing the restabilization of wakes. *AIAA 92-0067*.
- HINCH, E.J. 1991 *Perturbation Methods*. Cambridge: Cambridge University Press.
- HWANG, Y., KIM, J. & CHOI, H. 2013 Stabilization of absolute instability in spanwise wavy two-dimensional wakes. *Journal of Fluid Mechanics* **727**, 346–378.

- KIM, J. & CHOI, H. 2005 Distributed forcing of flow over a circular cylinder. *Physics of Fluids (1994-present)* **17** (3), –.
- MARQUET, O., SIPP, D. & JACQUIN, L. 2008 Sensitivity analysis and passive control of cylinder flow. *Journal of Fluid Mechanics* **615**, 221–252.
- MELIGA, P., SIPP, D. & CHOMAZ, J.-M. 2010 Open-loop control of compressible afterbody flows using adjoint methods. *Physics of Fluids* **22** (5), 054109.
- MICHALKE, A. 1964 On the inviscid instability of the hyperbolic-tangent velocity profile. *Journal of Fluid Mechanics* **19**, 543–556.
- TAMMISOLA, O., GIANNETTI, F., CITRO, V. & JUNIPER, M. P. 2014 Second-order perturbation of global modes and implications for spanwise wavy actuation. *Journal of Fluid Mechanics* **755**, 314–335.
- TREFETHEN, L.N., TREFETHEN, A.E., REDDY, S.C. & DRISCOLL, T.A. 1993 Hydrodynamic stability without eigenvalues. *Science* **261** (5121), pp. 578–584.
- TREFETHEN, L. N. 2000 *Spectral Methods in MATLAB*. Philadelphia: SIAM.
- VILLERMAUX, E. 1998 On the role of viscosity in shear instabilities. *Physics of Fluids (1994-present)* **10** (2), 368–373.
- ZDRAVKOVICH, M.M. 1981 Review and classification of various aerodynamic and hydrodynamic means for suppressing vortex shedding. *Journal of Wind Engineering and Industrial Aerodynamics* **7** (2), 145 – 189.